

## OPTIMIZING THE ITO INTERCONNECTION LAYER FOR MONOLITHIC PEROVSKITE SILICON TANDEM SOLAR CELLS WITH HIGH SHORT-CIRCUIT CURRENTS OF 20 mA/cm<sup>2</sup>

Özde Şeyma Kabaklı<sup>1\*</sup>, Kaitlyn McMullin<sup>1</sup>, Leonard Tutsch<sup>1</sup>, Martin Bivour<sup>1</sup>, Oliver Fischer<sup>1,2</sup>, Alexander J. Bett<sup>1</sup>, Martin Hermle<sup>1</sup>, Jan Christoph Goldschmidt<sup>3</sup>, Stefan W. Glunz<sup>1,2</sup>, Juliane Borchert<sup>1,2</sup>, Patricia S. C. Schulze<sup>1</sup>

<sup>1</sup>Fraunhofer Institute for Solar Energy Systems, Heidenhofstr. 2, 79110 Freiburg, Germany

<sup>2</sup>University of Freiburg, Department of Sustainable Systems Engineering (INATECH), Emmy-Noether-Str. 2, 79108 Freiburg

<sup>3</sup>University of Marburg, Department of Physics, Renthof 7. 10, 35032 Marburg

\*Corresponding author: Özde Şeyma Kabaklı<sup>1</sup>, +49 761 4588-2447, oezde.seyma.kabakli@ise.fraunhofer.de

**ABSTRACT:** In 2-terminal perovskite silicon tandem solar cells the interconnection layer that electrically connects the top and bottom cells plays a pivotal role for reaching highest efficiency. Typically made from a transparent conductive oxide, its electrical properties determine series resistance losses and shunt resilience, while its optical properties determine via reflection and transmission the current matching between the sub-cells. In this study, ITO interconnection layers are optimized for two-terminal monolithic p-i-n perovskite silicon tandem solar cells with a flat front side and textured rear side silicon bottom solar cell. The oxygen gas flow ratio during the sputter process of interconnection ITO is varied between 0% and 12% in oxygen and argon mixed gas. The effect of the variation on the opto-electrical properties of ITO thin films and tandem solar cell parameters is investigated. Optimization of the oxygen flow rate during sputtering increased the absolute tandem efficiency from 27.1% to 28.9%, while reaching a significantly higher short-circuit current density of 20 mA/cm<sup>2</sup>.

**Keywords:** Perovskite, Silicon, Tandem, Interconnection, ITO, photovoltaics

## 1 INTRODUCTION

Monolithic two-terminal perovskite silicon tandem solar cells have the potential to reach 45.1% power conversion efficiency (PCE) by reducing thermalization losses<sup>[1]</sup>. In monolithic perovskite silicon tandem solar cells, indium tin oxide (ITO) is often used as the electrical interconnection layer of the two sub solar cells<sup>[2]</sup>. An interconnection ITO should (i) have high vertical conductivity to reduce series resistance losses, (ii) have low lateral conductivity to suppress leakage current by shunt pathways and (iii) cause only minor optical losses<sup>[3]</sup>. An approach to increase sheet resistance ( $R_{\text{sheet}}$ ) and decrease optical absorption of the ITO layers is to increase the oxygen flow rate during sputtering<sup>[4]</sup>. Depending on the specifics of the shunts, the contribution of the bottom cell to the lateral transport and other factors, a high sheet resistance of the recombination (interconnection) junction can mitigate the impact of sub-cell shorting in the presence of local shunt paths<sup>[5-7]</sup>.

The hydroxyl group concentration at the ITO surface is important as the binding mechanism for 2PACz self-assembling molecules involves binding with a covalent bond to the hydroxyl group at the surface and forming P-OH and P=O groups with H<sub>2</sub>O as a side product. The ITO surface activity can be increased via surface cleaning methods such as hydrofluoric acid and UV-Ozone treatment<sup>[8]</sup>. Altering the ITO surface chemistry by oxygen flow might also influence the adsorption mechanism of the SAM by creating more stoichiometric oxide binding sites facilitating easy and strong adsorption.

This study investigates the effect of oxygen flow rate during the sputter process of the interconnection ITO in the tandem structure on solar cell parameters and assembly of 2PACz on ITO. The oxygen flow rate ratio during the sputter process is changed (0 sccm to 180 sccm) while keeping the thickness constant at 20 nm.

## 2 EXPERIMENTAL

### 2.1 Perovskite Silicon Tandem Solar Cells

Rear side textured, 250 µm thick p-type silicon float zone wafers (base resistivity 1 Ω cm) are used for fabrication of silicon heterojunction bottom solar cells. The rear side electrode consists of 195 nm ITO and 1000 nm Ag. Front side interconnection ITO thickness is 20 nm<sup>[9]</sup>. The ITO films are deposited in an industrial type in-line tool via DC sputtering from a rotary target. The oxygen flow rate during interconnection ITO sputtering is varied from 0% to 12% keeping the thickness constant. 2PACz is spin coated on the front ITO, followed by perovskite spin coating. 2PACz and perovskite solution preparation and deposition steps are done as described in ref<sup>[10]</sup>. LiF (1 nm) and C<sub>60</sub> (15 nm) are evaporated under high vacuum. SnO<sub>x</sub> (20 nm) is deposited using atomic layer deposition. Front side ITO (25 nm) is DC sputtered. Finally, Ag (200 nm) and MgF<sub>2</sub> (100 nm) are evaporated under high vacuum. Interconnection ITO, front side ITO and Ag depositions are fabricated using a shadow mask defining the individual active solar cell areas on substrates (4 solar cell of 0.25 cm<sup>2</sup> active area per substrate). All the steps of top solar cell processing, except the front side ITO sputtering, are carried out in inert atmosphere.

### 2.2 Characterization

Hall measurements are conducted to determine the electrical properties (sheet resistance, mobility, electron density) of the ITO thin films deposited on glass.

*I-V* measurements are done using a Wacom sun simulator consisting of a filtered Xenon (UV and visible light) and a filtered Halogen lamp (infrared light), and a Keithley 2400 source meter. Lamp intensities are adjusted using relative spectral response values per each solar cell group variation following the procedure described by Meusel et al.<sup>[10]</sup>. Measurements are performed in ambient air with the sample chuck temperature kept constant at 25 °C. EQE measurements of tandem solar cells are done using a chopped light (~130Hz frequency) of a Xenon lamp. The measurements of the perovskite and silicon sub-

solar cells are done separately by applying a bias voltage and bringing the measured sub-cell to current limitation by LED bias illumination. Detailed description of how tandem cells need to be measured can be found in [11–15]

The solar cell active area is defined by shadow masks during  $I$ - $V$  measurements.  $I$ - $V$  measurements are done under 1 sun illumination with a solar simulator with two lamps allowing for adjustment of the spectrum.

The series resistance of the tandem solar cells ( $R_{series}$ ) is calculated from the slope of the  $I$ - $V$  curve at  $V_{OC}$ .

Reflection measurements are conducted on full solar cells with the LOANA tool.

### 3 RESULTS

The oxygen flow rate during ITO thin film sputter process is varied between 0%-12% (oxygen percentage in oxygen and argon mixed gas). Hall measurements show that the sheet resistance increased from 392  $\Omega$ /sq to 10700 $\Omega$ /sq. The increase in the sheet resistance is dominated by the decrease in electron density, while highest mobility is obtained with 5% oxygen flow rate (Figure 1).

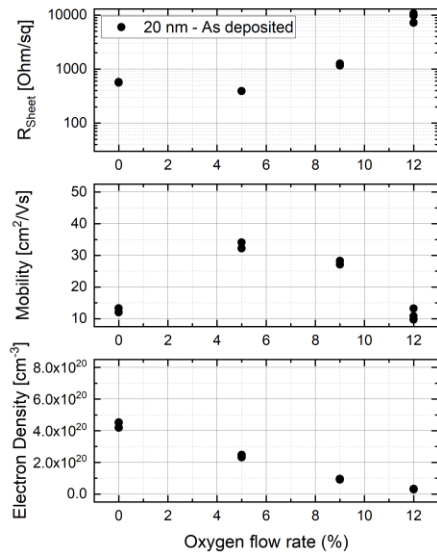


**Figure 1:** The flow rate of oxygen during sputtering of the as-deposited interconnection ITO on glass is varied between 0%-12%. Sheet resistance increases as the oxygen flow rate increases from 0% up to 12% Highest mobility is obtained for 5% oxygen flow rate. Highest electron density is obtained for 0%.

The 20 nm ITO thin films with 0%, 5%, 9% and 12% oxygen flow rate and  $R_{Sheet}$  of 575  $\Omega$ /sq, 392  $\Omega$ /sq, 1260  $\Omega$ /sq, 10700  $\Omega$ /sq on glass are implemented in perovskite silicon tandem solar cells, respectively (Figure 2).

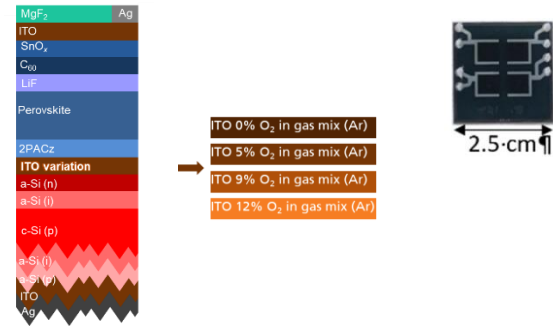


**Figure 2:** Perovskite silicon tandem solar cell sketch (left) with self-assembling molecular layer as hole transport layer and a thin LiF passivation at the electron transport layer-perovskite interface. Oxygen flow rate during sputtering of ITO interconnection layer is varied while keeping the rest constant. Each substrate (2.5 cm x 2.5 cm) has 4 solar cells with active areas (0.25  $cm^2$ ), defined by a shadow mask that is used during processing (right).

The normalized EQEs of the highest efficiency solar cell per group show small changes for 5% and 9% oxygen flow rate ITO compared to 0% and 12% for the silicon sub-cell. In the normalized EQE graph, between 900-1100 nm wavelength range, a negligible change in the shape is observed. Reflection losses of 5% group is lower compared to other oxygen flow rate groups at 1100-1200 nm wavelength range. The perovskite silicon tandem solar cell with 9% oxygen flow rate ITO interconnection layer has the highest  $iV_{OC}$  (Figure 3).

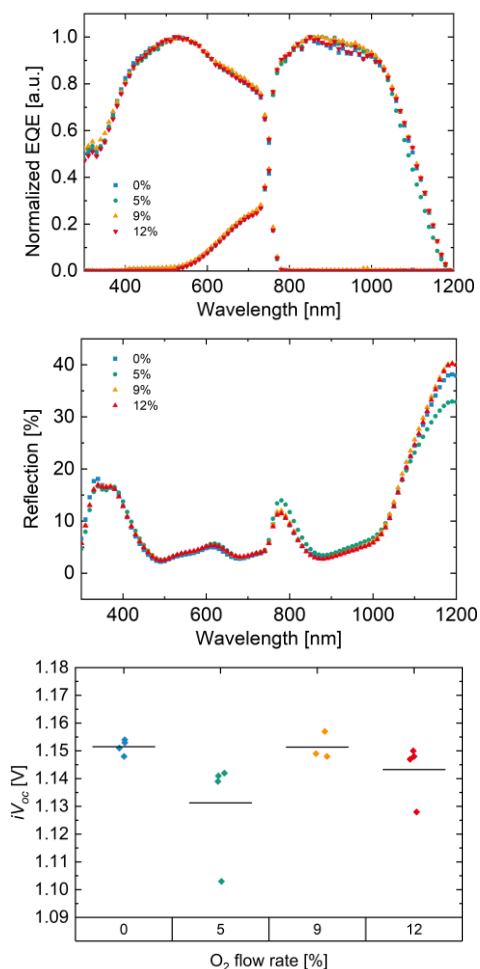


**Figure 3:** 2-terminal monolithic perovskite silicon tandem solar cell EQE is normalized to a maximum value of 1 (a), reflection at high wavelengths is reduced for 5% oxygen flow (b),  $iV_{oc}$  changed depending on the oxygen flow rate(c).

There is large spread within each  $I-V$  data group, a trend of increasing average  $j_{sc}$  from 9% to 12% oxygen flow can be observed. The highest average  $j_{sc}$ ,  $20.2 \text{ mA/cm}^2$  in forward scan and  $20.1 \text{ mA/cm}^2$  in reverse scan, is obtained with the highest oxygen flow group of 12% oxygen flow. In a previous study a similar tandem solar cell with 5% oxygen flow rate for the ITO interconnection layer was shown to be almost current matched with a slightly lower current from the bottom solar cell[10]. Taking this into consideration the increase of the short circuit current might be related to higher bottom solar cell current with increased transparency of the ITO interconnection layer with higher oxygen flow rate. More efficient infrared light harvesting can be expected if the reduced parasitic absorption by increasing the oxygen flow rate is the dominating optical effect. However, the trend in reflection does not follow the oxygen flow rate (Figure 3). Even though the parasitic absorption might be lower for higher oxygen flow rates, a significant change of the parasitic absorption of the ITO layer above 5% oxygen flow rate is not expected. One other optical reason for such a trend can be increasing refractive index for higher oxygen flow rates. Spectrometric characterization is necessary to investigate

if there are any changes in current matching point or if there are any other effects dominating [10–12]. Both 9% and 12% groups can achieve power conversion efficiencies above 26% (Figure 4). The absolute  $V_{oc}$  exhibits an upwards trend for higher  $O_2$  flow rates, whereas the average is around  $1.825 \text{ V}$  for all groups due to large data spread. One of the reasons for the increasing absolute  $V_{oc}$  could be reduced non-radiative recombination, which can be observed by  $iV_{oc}$  determined by PLQY measurements on tandem solar cells. Overall, highest stabilized power conversion efficiency over 3 minutes, 28.9%,  $20.03 \text{ mA/cm}^2 j_{sc}$ ,  $1.85 \text{ V } V_{oc}$ , and 78%  $FF$  is obtained with 9% oxygen flow rate with in-house measurements. The first two groups have less data points due to a smaller number of samples available. We are currently working on further data collection.

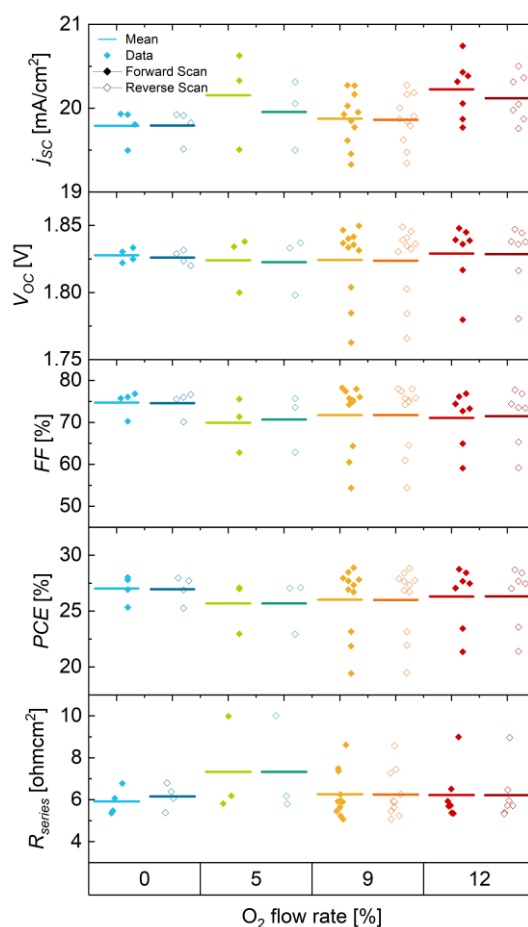


**Figure 4:**  $I-V$  data of the perovskite silicon tandem solar cells. Highest mean  $j_{sc}$  is obtained for 12% oxygen flow rate. High PCE above 27% is obtained for 9% and 12% oxygen flow.

As mentioned in the experimental details, the ITO interconnection layer is subjected to UV-ozone treatment before the 2PACz spin coating. The UV-Ozone treatment of the ITO surface might have a stronger influence on the surface chemistry of the 2PACz compared to the sputter gas oxygen flow rate. One possible reason for not observing a significant trend between the groups might be the dominating effect of the UV-ozone treatment on the surface chemistry of ITO.

The highest efficiency solar cell from the group with 9% oxygen flow was measured at Fraunhofer ISE CalLab PV Cells and 27.1% power conversion efficiency was certified. One of the reasons for lower power conversion efficiency result compared to in-house measurements could be LiF induced degradation of the perovskite top solar cell stack over time.

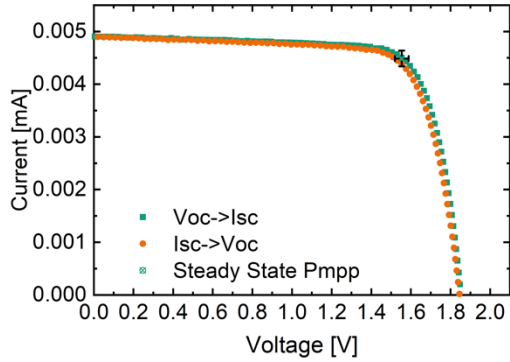


**Figure 4:** The highest efficiency solar cell was sent to CalLab at Fraunhofer ISE for certification three weeks later than the initial  $I$ - $V$  measurements. Some degradation effect is observed over the weeks.

A summary of the certified result can be found in Table 1. The solar cell shows almost no hysteresis.

**Table 1:** Solar cell parameters from the CalLab. The steady state PCE at maximum power point (MPP) is certified as  $27.1 \pm 1.2\%$ .

	Forward Scan		Reverse Scan	
$V_{OC}$	$1845 \pm 19$	mV	$1853 \pm 19$	mV
$I_{SC}$	$4.900 \pm 0.094$	mA	$4.908 \pm 0.094$	mA
$I_{MPP}$	4.46	mA	4.50	mA
$V_{MPP}$	1530	mV	1553	mV
$P_{MPP}$	6.83	mW	6.99	mW
FF	75.5	%	76.9	%
PCE				
Steady State MPP				
$I_{MPP}$	$4.49 \pm 0.15$	mA		
$V_{MPP}$	$1553 \pm 35$	mV		
$P_{MPP}$	$6.97 \pm 0.29$	mW		
FF				
PCE	$27.1 \pm 1.2$	%		

The highest efficiency solar cell was measured in-house over 10 days. The power conversion efficiency decreased by 1% over the 10 days (Figure 5).

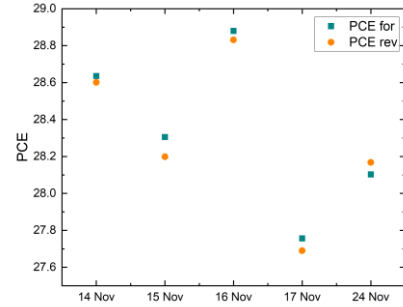


**Figure 5:** The in-house  $I$ - $V$  measurements of the highest efficiency solar cell over 10 days. The degradation of the solar cells might be related with the LiF passivation interlayer. The migration of  $Li^+$  and  $F^-$  ions might deteriorate the  $C_{60}$  interface [16, 17]. We are currently performing long term stability tests to understand the instability behaviour of the solar cells.

#### 4 DISCUSSION and CONCLUSION

In this study, oxygen flow rate during sputtering is varied between 0% to 12% for the perovskite silicon tandem solar cells ITO interconnection layer. The increase from 0% to 12% resulted in a slight upward trend in  $j_{sc}$ . The slight changes in  $j_{sc}$  could be related to a change in tandem current matching condition due to a decreased absorption with higher oxygen flow rate or change in the refractive index. Implied open-circuit voltage ( $iV_{OC}$ ) results suggest that the ITO interconnection layer oxygen flow rate could additionally influence the non-radiative recombination in the tandem solar cell. Also, the slope from  $j_{sc}$  to  $j_{MPP}$  could be an indication of parallel resistance problems and non-homogeneity of SAM binding over the active area. The bridging hydroxyl groups, spanning two or more metal sites, cause looser binding of the adsorbed SAMs on the surface compared to the terminal hydroxyl groups, that bond to a single metal atom site. The loosely bind SAMs can easily be disconnected from the ITO surface, which result in small pin-holes and induce current leakage<sup>[8]</sup>. The non-homogeneity might be due to non-sufficient terminal hydroxyl groups in the ITO surface, also reducing the fabrication yield of results. However, in the 0%-12% range, no clear trend or significant influence of the oxygen flow rate can be observed in solar cell parameters. There is also no direct correlation found between higher sheet resistance of the ITO interconnection layer and shunt quenching<sup>[6]</sup>. This might indicate that either there are no dominant losses caused by local shunts or the increasing series resistance did not have significant impact on shunt quenching.

To address these questions, spectrometric characterization<sup>[11, 12]</sup> and PL imaging is planned as next steps. Moreover, the effect of higher oxygen flow rates on 2PACz assembly on ITO surface is currently under investigation. All in all, it is shown that with our optimizations, very high short-circuit current density, of  $20 \text{ mA/cm}^2$  and high efficiency of 28.9% can be achieved. In order to reach higher efficiency and stability, the loss mechanisms at the interfaces will be addressed in further studies, such as implementing  $MgF_2$  or  $Al_2O_3$  as the passivation interlayer instead of LiF<sup>[17]</sup>.

## 5 ACKNOWLEDGEMENTS

This work was supported by Fraunhofer Gesellschaft, Germany via the Fraunhofer MANITU Lighthouse Project. Ö.Ş.K. gratefully acknowledges scholarship from the Dr. Ruth Heerdt Stiftung.

## 6 REFERENCES

- [1] M. H. Futscher and B. Ehrler, "Efficiency Limit of Perovskite/Si Tandem Solar Cells," *ACS Energy Letters*, vol. 1, no. 4, pp. 863–868, 2016, doi: 10.1021/acsenergylett.6b00405.
- [2] C. Li, Y. Wang, and Choy, Wallace C. H., "Efficient Interconnection in Perovskite Tandem Solar Cells," *Small Methods*, vol. 4, no. 7, p. 2000093, 2020, doi: 10.1002/smt.202000093.
- [3] Y. Ko, H. Park, C. Lee, Y. Kang, and Y. Jun, "Recent Progress in Interconnection Layer for Hybrid Photovoltaic Tandems," *Advanced materials (Deerfield Beach, Fla.)*, vol. 32, no. 51, e2002196, 2020, doi: 10.1002/adma.202002196.
- [4] A. Chen, K. Zhu, H. Zhong, Q. Shao, and G. Ge, "A new investigation of oxygen flow influence on ITO thin films by magnetron sputtering," *EuroSun2004*, vol. 120, pp. 157–162, 2014, doi: 10.1016/j.solmat.2013.08.036.
- [5] K. O. Brinkmann *et al.*, "Perovskite-organic tandem solar cells with indium oxide interconnect," *Nature*, vol. 604, no. 7905, pp. 280–286, 2022, doi: 10.1038/s41586-022-04455-0.
- [6] C. Blaga, G. Christmann, M. Boccard, C. Ballif, S. Nicolay, and B. Kamino, "Palliating the efficiency loss due to shunting in perovskite/silicon tandem solar cells through modifying the resistive properties of the recombination junction," *Sustainable Energy Fuels*, 2021, doi: 10.1039/D1SE00030F.
- [7] F. Ventosinos, J. Klusacek, T. Finsterle, K. Kunzel, F.-J. Haug, and J. Holovsky, "Shunt Quenching and Concept of Independent Global Shunt in Multijunction Solar Cells," *IEEE Journal of Photovoltaics*, vol. 8, no. 4, pp. 1005–1010, 2018, doi: 10.1109/JPHOTOV.2018.2828850.
- [8] M. Wu *et al.*, "Reconstruction of the Indium Tin Oxide Surface Enhances the Adsorption of High-Density Self-Assembled Monolayer for Perovskite/Silicon Tandem Solar Cells," *Advanced Functional Materials*, 2023, doi: 10.1002/adfm.202304708.
- [9] P. S. C. Schulze *et al.*, "25.1% High-Efficient Monolithic Perovskite Silicon Tandem Solar Cell with a High Band Gap Perovskite Absorber," *Solar RRL*, vol. 4, no. 7, p. 2000152, 2020, doi: 10.1002/solr.202000152.
- [10] M. Heydarian *et al.*, "Maximizing Current Density in Monolithic Perovskite Silicon Tandem Solar Cells," *Sol. RRL*, vol. 7, no. 7, p. 2200930, 2023, doi: 10.1002/solr.202200930.
- [11] A. J. Bett *et al.*, "Spectrometric Characterization of Monolithic Perovskite/Silicon Tandem Solar Cells," *Sol. RRL*, 2022, doi: 10.1002/solr.202200948.
- [12] M. Meusel, R. Adelhelm, F. Dimroth, A. W. Bett, and W. Warta, "Spectral mismatch correction and spectrometric characterization of monolithic III-V multi-junction solar cells," *Progress in Photovoltaics: Research and Applications*, vol. 10, no. 4, pp. 243–255, 2002, doi: 10.1002/pip.407.
- [13] M. Meusel, C. Baur, G. Létay, A. W. Bett, W. Warta, and E. Fernandez, "Spectral response measurements of monolithic GaInP/Ga(In)As/Ge triple-junction solar cells: Measurement artifacts and their explanation," *Progress in Photovoltaics: Research and Applications*, vol. 11, no. 8, pp. 499–514, 2003, doi: 10.1002/pip.514.
- [14] M. Saliba and L. Etgar, "Current Density Mismatch in Perovskite Solar Cells," *ACS Energy Lett.*, vol. 5, no. 9, pp. 2886–2888, 2020, doi: 10.1021/acsenergylett.0c01642.
- [15] M. Mundus *et al.*, "Spectrally resolved nonlinearity and temperature dependence of perovskite solar cells," *Solar Energy Materials and Solar Cells*, vol. 172, pp. 66–73, 2017, doi: 10.1016/j.solmat.2017.07.013.
- [16] A. Al-Ashouri *et al.*, "Monolithic perovskite/silicon tandem solar cell with 29% efficiency by enhanced hole extraction," *Science (New York, N.Y.)*, vol. 370, no. 6522, pp. 1300–1309, 2020, doi: 10.1126/science.abd4016.
- [17] J. Liu *et al.*, "Efficient and stable perovskite-silicon tandem solar cells through contact displacement by MgFx," *Science (New York, N.Y.)*, vol. 377, no. 6603, pp. 302–306, 2022, doi: 10.1126/science.abn8910.